CHAPTER

Texture 8

It is quite easy to understand what a texture is, although somewhat less easy to define it. For many reasons it is useful to be able to classify textures and to distinguish them from one another; it is also useful to be able to determine the boundaries between different textures, as they often signify the boundaries of real objects. This chapter studies the means for achieving these aims.

Look out for:

- basic measures by which textures can be classified—such as regularity, randomness, and directionality.
- problems that arise with "obvious" texture analysis methods, such as autocorrelation.
- the long-standing graylevel co-occurrence matrix method.
- Laws' method and Ade's generalization of it.
- the fact that textures have to be analyzed statistically, because of the random element in their construction.

Texture analysis is a core element in the vision repertoire, just as textures are core components of most images. It therefore seemed most appropriate to include this topic in Part 1 of the book.

8.1 INTRODUCTION

In the foregoing chapters, many aspects of image analysis and recognition have been studied. At the core of these matters has been the concept of segmentation, which involves the splitting of images into regions that have some degree of

uniformity, whether in intensity, color, texture, depth, motion, or other relevant attributes. Care has been taken in Chapter 4 to emphasize that such a process will be largely *ad hoc*, since the boundaries produced will not necessarily correspond to those of real objects. Nevertheless, it is important to make the attempt, either as a preliminary to more accurate or iterative demarcation of objects and their facets, or as an end in itself—e.g., to judge the quality of surfaces.

In this chapter, we move on to the study of texture and its measurement. Texture is a difficult property to define: indeed, in 1979, Haralick reported that no satisfactory definition of it had up till then been produced. Perhaps we should not be surprised by this, as the concept has rather separate meanings in the contexts of vision, touch, and taste: furthermore, the ways in which different people understand the terms are highly individual and subjective. Nevertheless, we require a working definition of texture, and in vision the particular aspect we focus on is the variation in intensity of a particular surface or region of an image. Even with this statement we are being indecisive about whether it is the physical object being observed which is being described or the image derived from it. This reflects the fact that it is the roughness of the surface or the structure or composition of the material that originally gives rise to its visual properties. However, in this chapter, we are mainly interested in the interpretation of images, and so we define texture as the characteristic variation in intensity of a region of an image, which should allow us to recognize and describe it and to outline its boundaries (Fig. 8.1).

This definition of texture implies that texture is nonexistent in a surface of uniform intensity and does not say anything about how the intensity might be expected to vary or how we might recognize and describe it. In fact, there are many ways in which intensity might vary, but if the variation does not have sufficient uniformity, the texture may not be characterized sufficiently close to permit recognition or segmentation.

We next consider ways in which intensity might vary. Clearly, it can vary rapidly or slowly, markedly or with low contrast, with a high or low degree of directionality, and with greater or lesser degrees of regularity. This last characteristic is often taken as key: either the textural pattern is regular as for a piece of cloth, or it is random as for a sandy beach or a pile of grass cuttings. However, this ignores the fact that a regular textural pattern is often not wholly regular (again, as for a piece of cloth), or not wholly random (as for a mound of potatoes of similar size). Thus, the degrees of randomness and of regularity will have to be measured and compared when characterizing a texture.

There are more profound things to say about the textures described earlier in this section. Often textures are derived from tiny objects or components that are themselves similar, but that are placed together in ways ranging from purely random to purely regular—be they bricks in a wall, grains of sand, blades of grass, strands of material, stripes on a shirt, wickerwork on a basket, or a host of other items. In texture analysis it is useful to have a name for the similar textural

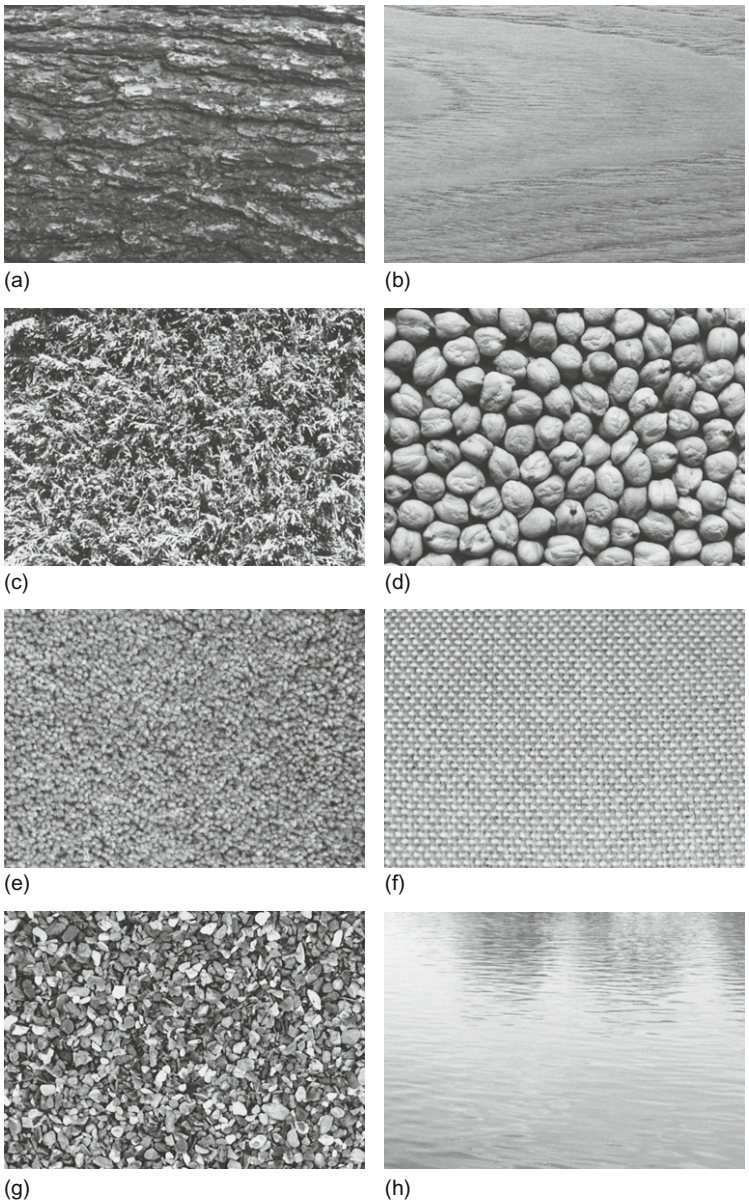

FIGURE 8.1

The variety of textures obtained from real objects. (a) Bark, (b) wood grain, (c) fir leaves, (d) chick peas, (e) carpet, (f) fabric, (g) stone chips, (h) water. These textures demonstrate the wide variety of familiar textures that are easily recognized from their characteristic intensity patterns.

elements that are replicated over a region of the image: such textural elements are called *texels*. These considerations lead us to characterize textures in the following ways:

1. The texels will have various sizes and degrees of uniformity.
2. The texels will be orientated in various directions.
3. The texels will be spaced at varying distances in different directions.
4. The contrast will have various magnitudes and variations.
5. Various amounts of background may be visible between texels.
6. The variations composing the texture may each have varying degrees of regularity *vis-à-vis* randomness.

It is quite clear from this discussion that a texture is a complicated entity to measure. The reason is primarily that many parameters are likely to be required to characterize it: in addition, when so many parameters are involved, it is difficult to disentangle the available data and measure the individual values or decide the ones that are most relevant for recognition. And of course, the statistical nature of many of the parameters is by no means helpful. However, we have so far only attempted to show how complex the situation can be. In what follows, we attempt to show that quite simple measures can be used to recognize and segment textures in practical situations.

Before proceeding, it is useful to recall that in the analysis of shape, there is a dichotomy between available analysis methods. We could, e.g., use a set of measures such as circularity, aspect ratio, and so on, which would permit a description of the shape, but which would not allow it to be reconstructed; or else we could use descriptors such as skeletons with distance function values, or moments, which would permit full and accurate reconstruction—although the set of descriptors might have been curtailed so that only limited but predictable accuracy was available. In principle, such a reconstruction criterion should be possible with texture. However, in practice there are two levels of reconstruction. In the first, we could reproduce a pattern which, to human eyes, would be indistinguishable from the off-camera texture until one compared the two on a pixel-by-pixel basis. In the second, we could reproduce a textured pattern exactly. The point is that textures are normally partially statistical in nature, so it will not be easy to obtain a pixel-by-pixel match in intensities: nor, in general, will it be worth aiming to do so. Thus, texture analysis generally only aims at obtaining accurate statistical descriptions of textures, from which *apparently* identical textures can be reproduced, if desired.

Very many workers have contributed to, and used, a wide range of approaches for texture analysis over a period of 40 years. The sheer weight of the available material and the statistical nature of it can be daunting for many. Note that Section 8.4 is particularly relevant to practitioners because it describes the Laws' texture energy approach which is intuitive, straightforward to apply in both software and hardware, and highly effective in many application areas. However, Section 8.3 on graylevel co-occurrence matrices (which were important historically) can be omitted on a first reading.

8.2 SOME BASIC APPROACHES TO TEXTURE ANALYSIS

In Section 8.1, texture was defined as the characteristic variation in intensity of a region of an image that should allow us to recognize and describe it and to outline its boundaries. In view of the likely statistical nature of textures, this prompts us to characterize texture by the variance in intensity values taken over the whole region of the texture.[1] However, such an approach will not give a rich enough description of the texture for most purposes and will certainly not provide any possibility of reconstruction: it will also be especially unsuitable in cases where the texels are well defined, or where there is a high degree of periodicity in the texture. On the other hand, for highly periodic textures such as that arise with many textiles, it is natural to consider the use of Fourier analysis. Indeed, in the early days of image analysis, this approach was tested thoroughly, although the results were not always encouraging.

Bajcsy (1973) used a variety of ring and orientated strip filters in the Fourier domain to isolate texture features—an approach that was found to work successfully on natural textures such as grass, sand, and trees. However, there is a general difficulty in using the Fourier power spectrum in that the information is more scattered than might be expected at first. In addition, strong edges and image boundary effects can prevent accurate texture analysis by this method. Perhaps more important is the fact that the Fourier approach is a global one that is difficult to apply successfully to an image that is to be segmented by texture analysis (Weszka et al., 1976).

Autocorrelation is another obvious approach to texture analysis, since it should show up both local intensity variations and also the repeatability of the texture (see Fig. 8.2). An early study was carried out by Kaizer (1955). He examined how many pixels an image has to shift before the autocorrelation function drops to $1/e$ of its initial value and produced a subjective measure of coarseness on this basis. However, Rosenfeld and Troy (1970a, 1970b) later showed that autocorrelation is not a satisfactory measure of coarseness. In addition, autocorrelation is not a very good discriminator of isotropy in natural textures. Hence, workers were quick to take up the co-occurrence matrix approach introduced by Haralick et al. (1973): in fact, this approach not only replaced the use of autocorrelation but during the 1970s also became to a large degree the "standard" approach to texture analysis.

8.3 GRAYLEVEL CO-OCCURRENCE MATRICES

The graylevel co-occurrence matrix approach[2] is based on studies of the statistics of pixel intensity distributions. As hinted above with regard to the variance in

[1] We defer for now the problem of finding the region of a texture so that we can compute its characteristics in order to perform a segmentation function. However, some preliminary training of a classifier may clearly be used to overcome this problem for supervised texture segmentation tasks.
[2] This is also frequently called the spatial graylevel dependence matrix (SGLDM) approach.

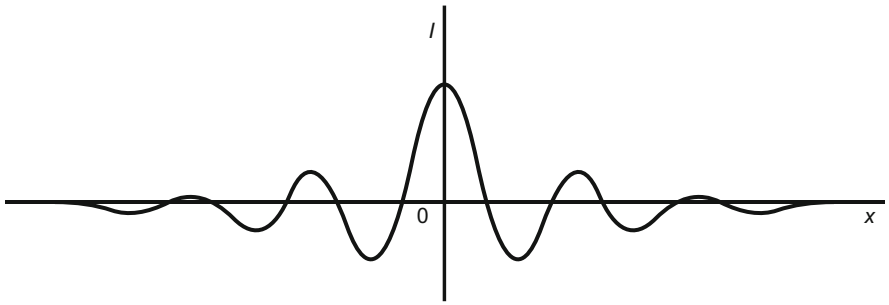

FIGURE 8.2

Use of autocorrelation function for texture analysis. This diagram shows the possible 1-D profile of the autocorrelation function for a piece of material in which the weave is subject to significant spatial variation: note that the periodicity of the autocorrelation function is damped down over quite a short distance.

pixel intensity values, single-pixel statistics do not provide rich enough descriptions of textures for practical applications. Thus, it is natural to consider second-order statistics obtained by considering *pairs* of pixels in certain spatial relations to each other. Hence, co-occurrence matrices are used, which express the relative frequencies (or probabilities) $P(i, j|d,\theta)$ with which two pixels having relative polar coordinates (d, θ) appear with intensities i, j. The co-occurrence matrices provide raw numerical data on the texture, although this data must be condensed to relatively few numbers before it can be used to classify the texture. The early paper by Haralick et al. (1973) gave 14 such measures, and these were used successfully for classification of many types of material (including, e.g., wood, corn, grass, and water). However, Conners and Harlow (1980a) found that only five of these measures were normally used, *viz.* "energy," "entropy," "correlation," "local homogeneity," and "inertia" (note that these names do not provide much indication of the modes of operation of the respective operators).

To obtain a more detailed idea of the operation of the technique, consider the co-occurrence matrix shown in Fig. 8.3. This corresponds to a nearly uniform image containing a single region in which the pixel intensities are subject to an approximately Gaussian noise distribution, the attention being on pairs of pixels at a constant vector distance $\mathbf{d} = (d, \theta)$ from each other. Next, consider the co-occurrence matrix shown in Fig. 8.4, which corresponds to an almost noiseless image with several nearly uniform image regions. In this case, the two pixels in each pair may correspond either to the same image regions or to different ones, although if d is small they will only correspond to adjacent image regions. Thus, we have a set of N on-diagonal patches in the co-occurrence matrix, but only a limited number L of the possible number M of off-diagonal patches linking them, where $M = {}^{N}C_2$ and $L \leq M$ (typically L will be of order N rather than N^2). With textured images, if the texture is not too strong, it may be modeled as noise, and

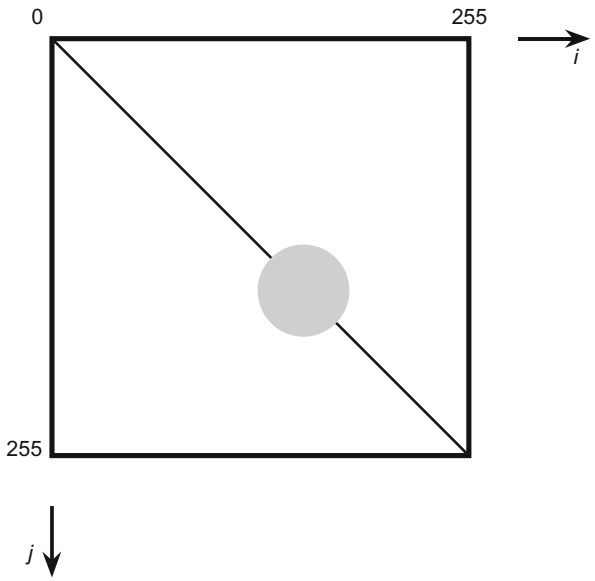

FIGURE 8.3

Co-occurrence matrix for a nearly uniform grayscale image with superimposed Gaussian noise. Here the intensity variation is taken to be almost continuous: normal convention is followed by making the *j* index increase downward, as for a table of discrete values (cf. Fig. 8.4).

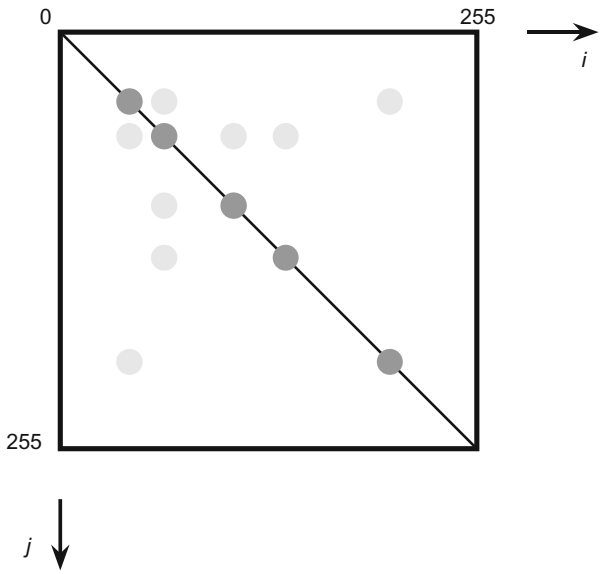

FIGURE 8.4

Co-occurrence matrix for an image with several distinct regions of nearly constant intensity. Again, the leading diagonal of the diagram is from top left to bottom right (cf. Figs. 8.2 and 8.5).

the $N + L$ patches in the image will be larger but still not overlapping. However, in more complex cases, the possibility of segmentation using the co-occurrence matrices will depend on the extent to which **d** can be chosen to prevent the patches from overlapping. Since many textures are directional, careful choice of θ will clearly help with this task, although the optimum value of d will depend on several other characteristics of the texture.

As a further illustration, we consider the small image shown in Fig. 8.5(a). To produce the co-occurrence matrices for a given value of **d**, we merely need to calculate the numbers of cases for which pixels, a distance **d** apart, have intensity values i and j. Here, we content ourselves with the two cases $\mathbf{d} = (1,\ 0)$ and $\mathbf{d} = (1, \pi/2)$. We thus obtain the matrices shown in Fig. 8.5(b) and (c).

This simple example demonstrates that the amount of data in the matrices is liable to be many times more than in the original image—a situation which is exacerbated in more complex cases by the number of values of d and θ that are required to accurately represent the texture. In addition, the number of gray levels will normally be closer to 256 than to 6, and the amount of matrix data varies as the square of this number. Finally, we should notice that the co-occurrence

(a)

0	0	0	1
1	1	1	1
2	2	2	3
3	3	4	5

(b)

	0	1	2	3	4	5
0	2	1	0	0	0	0
1	1	3	0	0	0	0
2	0	0	2	1	0	0
3	0	0	1	1	1	0
4	0	0	0	1	0	1
5	0	0	0	0	1	0

(c)

	0	1	2	3	4	5
0	0	3	0	0	0	0
1	3	1	3	1	0	0
2	0	3	0	2	1	0
3	0	1	2	0	0	1
4	0	0	1	0	0	0
5	0	0	0	1	0	0

FIGURE 8.5

Co-occurrence matrices for a small image. (a) The original image; (b) the resulting co-occurrence matrix for $\mathbf{d} = (1, 0)$; and (c) the matrix for $\mathbf{d} = (1, \pi/2)$. Note that even in this simple case, the matrices contain more data than the original image.

matrices merely provide a new representation: they do not themselves solve the recognition problem.

These factors mean that the gray scale has to be compressed into a much smaller set of values and careful choice of specific sample d, θ values must be made: in most cases, it is not at all obvious how such a choice should be made, and it is even more difficult to arrange for it to be made automatically. In addition, various functions of the matrix data must be tested before the texture can be properly characterized and classified.

These problems with the co-occurrence matrix approach have been tackled in many ways: just two are mentioned here. The first is to ignore the distinction between opposite directions in the image, thereby reducing storage by 50%. The second is to work with *differences* between gray levels; this amounts to performing a summation in the co-occurrence matrices along axes parallel to the main diagonal of the matrix. The result is a set of *first*-order *difference* statistics. While these modifications have given some additional impetus to the approach, the 1980s saw a highly significant diversification of methods for the analysis of textures. Of these, Laws' approach (1979, 1980a, 1980b) is important in that it has led to other developments which provide a systematic, adaptive means of tackling texture analysis. This approach is covered in Section 8.4.

8.4 LAWS' TEXTURE ENERGY APPROACH

In 1979 and 1980 Laws presented his novel texture energy approach to texture analysis (Laws, 1979, 1980a, 1980b). This involved the application of simple filters to digital images. The basic filters he used were common Gaussian, edge detector, and Laplacian-type filters, and were designed to highlight points of high "texture energy" in the image. By identifying these high energy points, smoothing the various filtered images, and pooling the information from them, he was able to characterize textures highly efficiently. As remarked earlier, Laws' approach has strongly influenced much subsequent work and it is therefore worth considering it here in some detail.

The Laws' masks are constructed by convolving together just three basic 1×3 masks:

$$L3 = \begin{bmatrix} 1 & 2 & 1 \end{bmatrix} \tag{8.1}$$

$$E3 = \begin{bmatrix} -1 & 0 & 1 \end{bmatrix} \tag{8.2}$$

$$S3 = \begin{bmatrix} -1 & 2 & -1 \end{bmatrix} \tag{8.3}$$

The initial letters of these masks indicate *L*ocal averaging, *E*dge detection, and *S*pot detection. In fact, these basic masks span the entire 1×3 subspace and form

Table 8.1 The Nine 3×3 Laws Masks

$L3^TL3$	$L3^TE3$	$L3^TS3$
$\begin{matrix} 1 & 2 & 1 \\ 2 & 4 & 2 \\ 1 & 2 & 1 \end{matrix}$	$\begin{matrix} -1 & 0 & 1 \\ -2 & 0 & 2 \\ -1 & 0 & 1 \end{matrix}$	$\begin{matrix} -1 & 2 & -1 \\ -2 & 4 & -2 \\ -1 & 2 & -1 \end{matrix}$
$E3^TL3$	$E3^TE3$	$E3^TS3$
$\begin{matrix} -1 & -2 & -1 \\ 0 & 0 & 0 \\ 1 & 2 & 1 \end{matrix}$	$\begin{matrix} 1 & 0 & -1 \\ 0 & 0 & 0 \\ -1 & 0 & 1 \end{matrix}$	$\begin{matrix} 1 & -2 & 1 \\ 0 & 0 & 0 \\ -1 & 2 & -1 \end{matrix}$
$S3^TL3$	$S3^TE3$	$S3^TS3$
$\begin{matrix} -1 & -2 & -1 \\ 2 & 4 & 2 \\ -1 & -2 & -1 \end{matrix}$	$\begin{matrix} 1 & 0 & -1 \\ -2 & 0 & 2 \\ 1 & 0 & -1 \end{matrix}$	$\begin{matrix} 1 & -2 & 1 \\ -2 & 4 & -2 \\ 1 & -2 & 1 \end{matrix}$

a complete set. Similarly, the 1×5 masks obtained by convolving pairs of these 1×3 masks together form a complete set:[3]

$$L5 = \begin{bmatrix} 1 & 4 & 6 & 4 & 1 \end{bmatrix} \tag{8.4}$$

$$E5 = \begin{bmatrix} -1 & -2 & 0 & 2 & 1 \end{bmatrix} \tag{8.5}$$

$$S5 = \begin{bmatrix} -1 & 0 & 2 & 0 & -1 \end{bmatrix} \tag{8.6}$$

$$R5 = \begin{bmatrix} 1 & -4 & 6 & -4 & 1 \end{bmatrix} \tag{8.7}$$

$$W5 = \begin{bmatrix} -1 & 2 & 0 & -2 & 1 \end{bmatrix} \tag{8.8}$$

In Eqs. (8.7) and (8.8), the initial letters indicate *R*ipple detection and *W*ave detection. We can also use matrix multiplication (see also Section 3.6) to combine the 1×3 and a similar set of 3×1 masks to obtain nine 3×3 masks—e.g.:

$$\begin{bmatrix} 1 \\ 2 \\ 1 \end{bmatrix} \begin{bmatrix} -1 & 2 & -1 \end{bmatrix} = \begin{bmatrix} -1 & 2 & -1 \\ -2 & 4 & -2 \\ -1 & 2 & -1 \end{bmatrix} \tag{8.9}$$

The resulting set of masks also forms a complete set (Table 8.1): note that two of these masks are identical to the Sobel operator masks. The corresponding 5×5 masks are entirely similar but are not considered in detail here as all relevant principles are illustrated by the 3×3 masks.

All such sets of masks include one whose components do not average to zero. Thus, it is less useful for texture analysis since it will give results dependent more on image intensity than on texture. The remainder are sensitive to edge points, spots, lines, and combinations of these.

[3] In principle nine masks can be formed in this way, but only five of them are distinct.

Having produced images that indicate, e.g., local edginess, the next stage is to deduce the local magnitudes of these quantities. These magnitudes are then smoothed over a fair-sized region rather greater than the basic filter mask size (e.g., Laws used a 15×15 smoothing window after applying his 3×3 masks): the effect of this is to smooth over the gaps between the texture edges and other microfeatures. At this point the image has been transformed into a vector image, each component of which represents energy of a different type. Although Laws (1980b) used both squared magnitudes and absolute magnitudes to estimate texture energy, the former correspond to true energy and give a better response, while the latter are useful in requiring less computation:

$$E(l,m) = \sum_{i=l-p}^{l+p} \sum_{j=m-p}^{m+p} |F(i,j)| \tag{8.10}$$

where $F(i, j)$ is the local magnitude of a typical microfeature, which is smoothed at a general scan position (l, m) in a $(2p + 1) \times (2p + 1)$ window.

A further stage is required to combine the various energies in a number of different ways, providing several outputs that can be fed into a classifier to decide upon the particular type of texture at each pixel location (Fig. 8.6). If necessary, principal components analysis is used at this point to help select a suitable set of intermediate outputs.

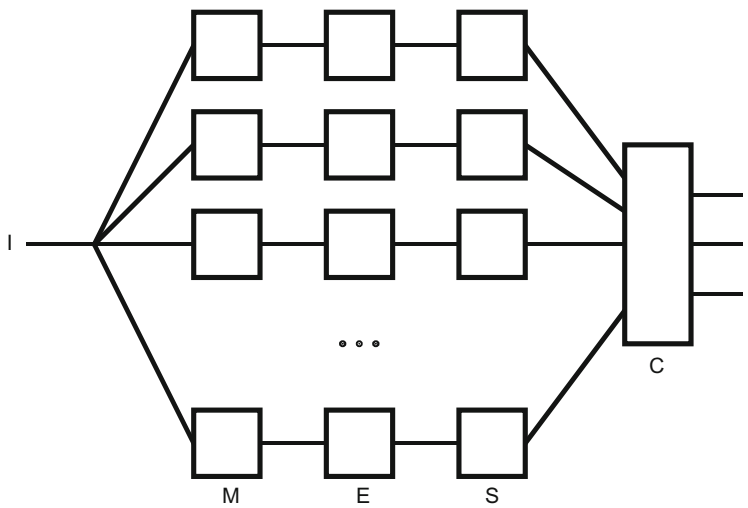

FIGURE 8.6

Basic form for a Laws' texture classifier. Here, I is the incoming image, M represents the microfeature calculation, E the energy calculation, S the smoothing, and C the final classification.

Laws' method resulted in excellent classification accuracy quoted at, e.g., 87% compared with 72% for the co-occurrence matrix method, when applied to a composite texture image of grass, raffia, sand, wool, pigskin, leather, water, and wood (Laws, 1980b). He also found that the histogram equalization normally applied to images to eliminate first-order differences in texture field grayscale distributions gave little improvement in this case.

Research was undertaken by Pietikäinen et al. (1983) to determine whether the precise coefficients used in the Laws' masks are responsible for the performance of his method. They found that so long as the general forms of the masks were retained, performance did not deteriorate, and could in some instances be improved. They were able to confirm that Laws' texture energy measures are more powerful than measures based on pairs of pixels (i.e., co-occurrence matrices).

8.5 ADE'S EIGENFILTER APPROACH

In 1983, Ade investigated the theory underlying the Laws' approach and developed a revised rationale in terms of eigenfilters.[4] He took all possible pairs of pixels within a 3×3 window, and characterized the image intensity data by a 9×9 covariance matrix. He then determined the eigenvectors required to diagonalize this matrix. These correspond to filter masks similar to the Laws' masks, i.e., use of these "eigenfilter" masks produces images that are principal component images for the given texture. Furthermore, each eigenvalue gives the part of the variance of the original image that can be extracted by the corresponding filter. Essentially, the variances give an exhaustive description of a given texture in terms of the texture of the images from which the covariance matrix was originally derived. Clearly, the filters that give rise to low variances can be taken to be relatively unimportant for texture recognition.

It will be useful to illustrate the technique for a 3×3 window. Here, we follow Ade (1983) in numbering the pixels within a 3×3 window in scan order:

1	2	3
4	5	6
7	8	9

This leads to a 9×9 covariance matrix for describing relationships between pixel intensities within a 3×3 window, as stated above. At this point, we recall that we are describing a texture and assuming that its properties are not synchronous with the pixel tessellation, we would expect various coefficients of the covariance matrix $\mathbf{C}$ to be equal: e.g., C_{24} should equal C_{57}; in addition, C_{57} must equal C_{75}.

[4]Before reading further, the reader may find it helpful to refer to Section 24.10, where principal components analysis and eigenvalue problems are discussed.

Table 8.2 Spatial Relationships Between Pixels in a 3×3 Window

a	*b*	*c*	*d*	*e*	*f*	*g*	*h*	*i*	*j*	*k*	*l*	*m*
9	6	6	4	4	3	3	1	1	2	2	2	2

This table shows the number of occurrences of the spatial relationships between pixels in a 3×3 window. Note that a is the diagonal element of the covariance matrix ***C****, and that all others appear twice as many times in* ***C*** *as indicated in the table.*

It is worth pursuing this matter, as a reduced number of parameters will lead to increased accuracy in determining the remaining ones. In fact, there are $9\ C_2 = 36$ ways of selecting pairs of pixels, but there are only 12 distinct spatial relationships between pixels if we disregard translations of whole pairs—or 13 if we include the null vector in the set (see Table 8.2). Thus, the covariance matrix (see Section 24.10), whose components include the 13 parameters a–m, takes the form:

$$\mathbf{C} = \begin{bmatrix} a & b & f & c & d & k & g & m & h \\ b & a & b & e & c & d & l & g & m \\ f & b & a & j & e & c & i & l & g \\ c & e & j & a & b & f & c & d & k \\ d & c & e & b & a & b & e & c & d \\ k & d & c & f & b & a & j & e & c \\ g & l & i & c & e & j & a & b & f \\ m & g & l & d & c & e & b & a & b \\ h & m & g & k & d & c & f & b & a \end{bmatrix} \tag{8.11}$$

C is symmetric, and the eigenvalues of a real symmetric covariance matrix are real and positive, and the eigenvectors are mutually orthogonal (see Section 24.10). In addition, the eigenfilters thus produced reflect the proper structure of the texture being studied and are ideally suited to characterizing it. For example, for a texture with a prominent highly directional pattern, there will be one or more high energy eigenvalues with eigenfilters having strong directionality in the corresponding direction.

8.6 APPRAISAL OF THE LAWS AND ADE APPROACHES

At this point, it will be worthwhile to compare the Laws and Ade approaches more carefully. In the Laws approach, standard filters are used, texture energy images are produced, and then principal component analysis may be applied to lead to recognition, whereas in the Ade approach, special filters (the eigenfilters) are applied, incorporating the results of principal component analysis, following

which texture energy measures are calculated, and a suitable number of these are applied for recognition.

The Ade approach is superior to the extent that it permits low-value energy components to be eliminated early on, thereby saving computation. For example, in Ade's application, the first five of the nine components contain 99.1% of the total texture energy, so the remainder can be ignored. In addition, it would appear that another two of the components containing respectively 1.9% and 0.7% of the energy could also be ignored, with little loss of recognition accuracy. However, in some applications textures could vary continually, and it may well be inadvisable to fine-tune a method to the particular data pertaining at any one time.[5]

In 1986, Unser developed a more general version of the Ade technique that also covered the methods of Faugeras (1978), Granlund (1980), and Wermser and Liedtke (1982). In this approach, performance is optimized not only for texture classification, but also for discrimination between two textures by simultaneous diagonalization of two covariance matrices. The method was developed further by Unser and Eden (1989, 1990): this work makes a careful analysis of the use of nonlinear detectors. As a result, two levels of nonlinearity are employed, one immediately after the linear filters are designed (by employing a specific Gaussian texture model) to feed the smoothing stage with genuine variance or other suitable measures, and the other after the spatial smoothing stage to counteract the effect of the earlier filter and aiming to provide a feature value that is in the same units as the input signal. In practical terms, this means having the capability for providing an RMS texture signal from each of the linear filter channels.

Overall, the originally intuitive Laws approach emerged during the 1980s as a serious alternative to the co-occurrence matrix approach. It is as well to note that alternative methods that are potentially superior have also been devised—see e.g., the local rank correlation method of Harwood et al. (1985), and the forced-choice method of Vistnes (1989) for finding edges between different textures, which apparently has considerably better accuracy than the Laws approach. Vistnes's (1989) investigation concludes that the Laws approach is limited by (a) the small scale of the masks that can miss larger-scale textural structures and (b) the fact that the texture energy smoothing operation blurs the texture feature values across the edge. The latter finding (or even the worse situation where a third class of texture appears to be located in the region of the border between two textures) has also been noted by Hsiao and Sawchuk (1989, 1990) who applied an improved technique for feature smoothing; they also used probabilistic relaxation for enforcing spatial organization on the resulting data.

[5]For example, these remarks apply (1) to textiles, for which the degree of stretch will vary continuously during manufacture, (2) to raw food products, such as beans, whose sizes will vary with the source of supply, and (3) to processed food products, such as cakes, for which the crumbliness will vary with cooking temperature and water vapor content.

8.7 CONCLUDING REMARKS

In this chapter, we have seen the difficulties of analyzing textures: these arise from the potential, and in many cases the frighteningly real complexities of textures—not least from the fact that their properties are often largely statistical in nature. The erstwhile widely used grayscale co-occurrence matrix approach has been seen to have distinct computational shortcomings. First, many co-occurrence matrices are in principle required (with different values of d and θ) in order to adequately describe a given texture; second, the co-occurrence matrices can be very large and, paradoxically, may hold more data than the images they are characterizing—especially if the range of grayscale values is large. In addition, many sets of co-occurrence matrices may be needed to allow for variation of the texture over the image, and if necessary, to initiate segmentation. Hence, co-occurrence matrices need to be significantly compressed, although in most cases it is not at all obvious *a priori* how this should be achieved, and it is even more difficult to arrange for it to be carried out automatically. This probably explains why attention shifted during the 1980s to other approaches, including particularly Laws' technique and its variations (especially that of Ade). Other developments were fractal-based measures, Markov approaches and the Gabor filter technique, although space has prevented a discussion of these methods here: see Section 8.8 for further reading on these topics.

Textures are recognized and segmented by humans with the same apparent ease as for plain objects. This chapter has shown that texture analysis needs to be sensitive to microstructures and then pulled into macrostructures—with PCA (principal components analysis) being a natural means of finding the optimum structure. The subject has great importance for new applications, such as iris recognition.

8.8 BIBLIOGRAPHICAL AND HISTORICAL NOTES

Early work on texture analysis was carried out by Haralick et al. (1973) and in 1976, Weska and Rosenfeld applied textural analysis to materials' inspection. The area was reviewed by Zucker (1976a) and Haralick (1979), and excellent accounts appear in the books by Ballard and Brown (1982) and Levine (1985).

At the end of the 1970s, the Laws technique (1979, 1980a, 1980b) arrived upon the scene (which had up till then been dominated by the co-occurrence matrix approach) and led to the principal components approach of Ade (1983), which was further developed by Dewaele et al. (1988), Unser and Eden (1989, 1990), and others. The direction taken by Laws was particularly valuable as it showed how texture analysis could be implemented straightforwardly and in a manner consistent with real-time applications such as inspection.

The 1980s also saw other new developments, such as the fractal approach led by Pentland (1984), and a great amount of work on Markov random field models of texture. Here the work of Hansen and Elliott (1982) was very formative, although the names G.R. Cross, H. Derin, D. Geman, S. Geman, and A.K. Jain come up repeatedly in this context. Bajcsy and Liebermann (1976), Witkin (1981), and Kender (1983) pioneered the *shape from texture* concept, which has received considerable attention ever since. Later, much work appeared on the application of neural networks to texture analysis, e.g., Greenhill and Davies (1993) and Patel et al. (1994). A number of reviews and useful comparative studies have been made including Van Gool et al. (1985), du Buf et al. (1990), Ohanian and Dubes (1992), and Reed and du Buf (1993). For further work on texture analysis related to inspection of faults and foreign objects, see Chapter 20.

More recent developments include further work with automated visual inspection in mind (Davies, 2000c; Tsai and Huang, 2003; Ojala et al., 2002; Manthalkar et al., 2003; Pun and Lee, 2003), although several of these papers also cite medical, remote sensing, and other applications. Of these papers, the last three are specifically aimed at rotation invariant texture classification and the last one also aims at scale invariance. In previous years, there has not been quite enough emphasis on rotation invariance, although it was by no means a new topic. Other work (Clerc and Mallat, 2002) was concerned with recovering shape from texture *via* a texture gradient equation, while Ma et al. (2003) were particularly concerned with person identification based on iris textures. Mirmehdi and Petrou (2000) described an in-depth investigation of color texture segmentation. In this context, the importance of "wavelets"[6] as an increasingly used technique of texture analysis with interesting applications (such as, human iris recognition) should be noted (e.g., Daugman, 1993, 2003).

Then, in a particularly exciting advance, Spence et al. (2004) managed to eliminate texture by using photometric stereo to find the underlying surface shape (or "bump map"), following which they were able to perform impressive reconstructions, including texture, from a variety of viewpoints; McGunnigle and Chantler (2003) have shown that this sort of technique is also able to reveal hidden writing on textured surfaces, where only pen pressure marks have been made. Similarly, Pan et al. (2004) have shown how texture can be eliminated from ancient tablets (in particular those made of lead and wood) to reveal clear images of the writing underneath.

8.8.1 More Recent Developments

Over the 2000s, the trend to scale and rotation invariant texture analysis mentioned above has continued, the paper by Janney and Geers (2010) describing an

[6]Wavelets are directional filters reminiscent of the Laws edges, bars, waves, and ripples, but have more rigorously defined shapes and envelopes, and are defined in multiresolution sets (Mallat, 1989).

"invariant features of local textures" approach, using a strictly circular 1-D array of sampling, positions around any given position. The method employs Haar wavelets and as a result is computationally efficient. It is applied at multiple scales in order to achieve scale invariance; in addition, intensity normalization is used to make the method illumination as well as scale and rotation invariant.

Two new books have recently been published on this rather specialist subject—by Petrou and Sevilla (2006) and Mirmehdi et al. (2008). The first is a very sound textbook, starting from a low level and progressing through topics not covered in the present volume, such as fractals, Markov random fields, Gibbs distributions, Gabor functions, wavelets, and the Wigner distribution. The second is an edited volume containing chapters by various researchers and providing much new information—as indicated by some of the more novel chapter titles: "TEXEMS: random texture representation and analysis," "3-D texture analysis," "Texture for appearance models," "From dynamic texture to dynamic shape and appearance models," "Divide-and-texture: Hierarchical feature description," "Practical implementation of the trace transform," and "Face analysis using local binary patterns."